

New insights on the physical Riemann surfaces of the ratio G_E^Λ/G_M^Λ

Francesco Rosini^{a,b,*} and Simone Pacetti^{a,b}

^a*Dipartimento di Fisica e Geologia, Università degli Studi di Perugia,
Via Alessandro Pascoli, Perugia, Italy*

^b*INFN, Sezione di Perugia,
Via Alessandro Pascoli, Perugia, Italy*

E-mail: francesco.rosini@pg.infn.it, simone.pacetti@unipg.it

The BESIII [1] and BaBar collaborations produced data suitable for the measurement of the Λ baryon electric and magnetic form factor's ratio G_E^Λ/G_M^Λ in the time-like region. By assuming the analyticity of the baryon form factors, a dispersive procedure can be used to analyze the data under a set of theoretical constraints. This procedure allows the behaviour of the modulus and the phase of the form factor's ratio in the time-like and space-like regions to be determined. Different classes of solutions are taken into account, and the results allow crucial properties of the baryon to be determined, such as the presence of zeroes of the form factor's ratio in the space-like region and the baryon's charge radius.

*Third Italian Workshop on the Physics at High Intensity (WIFAI2024)
12-15 November 2024
Bologna, Italy*

*Speaker

1. Introduction

The form factors (FFs) are Lorentz scalar functions of the squared four-momentum transfer which describe the internal properties of baryons, such as the Λ particle.

Two independent FFs, the Pauli and Dirac FFs, F_1 and F_2 , are required to describe the $\Lambda\Lambda\gamma$ vertex. They represent the spin-conserving and the spin-flipping part of the interaction. The expectation value of the hadronic current J_{had}^μ in a scattering process can be expressed in terms of the FFs as

$$\langle N(p') | J_{\text{had}}^\mu | N(p) \rangle = \bar{u}(p') \left[\gamma^\mu F_1(q^2) + \frac{i\sigma^{\mu\nu} q_\nu}{2M_B} F_2(q^2) \right] u(p), \quad (1)$$

where $|N(p)\rangle$ is the entering baryon's state of four-momentum p^μ , $u(p)$ is the corresponding Dirac spinor, M_B is the baryon's mass and q^2 is the four-momentum transfer, while p'^μ accounts for the exiting baryon. The most used FFs are the Sachs FFs G_E and G_M defined as

$$\begin{aligned} G_E(q^2) &= F_1(q^2) - \frac{q^2}{2M_B} F_2(q^2), \\ G_M(q^2) &= F_1(q^2) + F_2(q^2), \end{aligned} \quad (2)$$

and they assume an immediate interpretation in the Breit frame, where they are the Fourier transforms of the electric and magnetic charge densities respectively. The relative phase between the electric and magnetic FFs, $\arg(G_E^\Lambda/G_M^\Lambda)$, is directly related to their polarization, so the FFs ratio $R(q^2) = G_E^\Lambda(q^2)/G_M^\Lambda(q^2)$ is a crucial quantity to be studied.

We use a dispersive approach, based on first principles and theoretical constraints, to analyze the experimental data on the ratio G_E^Λ/G_M^Λ . This procedure is able to find the specific determination in which the phase is lying, i.e. the Riemann surface to which the physical values of the ratio belong.

The FFs are analytic functions in the q^2 complex plane with a branch cut along the positive direction of the real axis, originating from the theoretical threshold, $q^2 = q_{\text{th}}^2$, up to infinity. The theoretical threshold for the isoscalar final state $\Lambda\bar{\Lambda}$ is represented by the lightest isoscalar state, which is the three-pion state $\pi^+\pi^-\pi^0$, setting the theoretical threshold to $q_{\text{th}}^2 = (2M_\pi + M_{\pi^0})^2$.

The values accessible by experiments are only in the time-like region of the q^2 complex plane, where the Λ FFs have generally a non-zero imaginary part. Moreover, only data for center-of-mass energies $q^2 \geq q_{\text{phy}}^2 = (2M_\Lambda)^2$ can be accessed. The subsequent weak decay $\Lambda \rightarrow p\pi^- + c.c.$ is commonly exploited to identify the baryon thanks to the charged products of the decay. For this reason, it is possible to extract the relative phase $\arg(G_E^\Lambda/G_M^\Lambda)$ without directly measuring the polarization.

From the y-component of polarization vector's formula for the outgoing baryon B ,

$$\mathcal{P}_y = - \frac{\sqrt{\frac{q^2}{4M_B^2} \frac{|G_E^\Lambda|}{|G_M^\Lambda|}} \sin(2\theta) \sin(\arg(G_E^\Lambda/G_M^\Lambda))}{\frac{q^2}{4M_B^2} (1 + \cos^2(\theta)) + \frac{|G_E^\Lambda|^2}{|G_M^\Lambda|^2} \sin^2(\theta)}, \quad (3)$$

where θ is the scattering angle in the e^+e^- center-of-mass frame, we can see that the experimental data do not give any clue on the determination of the relative phase and the information it contains, since this quantity is measured through its sine, hence the relative phase is given as an angle in the range $[-\pi, \pi]$.

2. Data selection

The data sets used for this analysis have been obtained by the BaBar experiment in 2007 [2] and by the BESIII experiment in 2019 [3]. In total, there are three experimental points for the modulus and two for the relative phase of the ratio $R(q^2)$. The BaBar data are affected by lower statistics, while the BESIII data are more precise due to being obtained by a direct measurement, extracted by the collected events $e^+e^- \rightarrow \Lambda\bar{\Lambda}$ at the desired energy.

3. Dispersion relations for G_E^Λ/G_M^Λ

In the case of FFs, an analytic-continuation technique such as the dispersion relations (DRs) proves very useful. The function we consider is the FFs ratio $R(q^2)$, whose analytic properties can be derived from the ones of the electric G_E^Λ and the magnetic G_M^Λ FFs.

Analyticity domain The ratio is a multivalued meromorphic function on the same analyticity domain of the FFs, with a set of poles corresponding to the zeroes of the magnetic FF G_M^Λ , that are not cancelled by higher order zeroes of the electric FF G_E^Λ . Assuming that the magnetic FF has no zeroes, the analyticity domain of the ratio corresponds to the one of the FFs. Moreover, from the normalization of the FFs at $q^2 = 0$, it follows that

$$\begin{aligned} G_E^\Lambda(0) &= Q_\Lambda = 0, \\ G_M^\Lambda(0) &= \mu_\Lambda = -0.613 \pm 0.004 \mu_N, \end{aligned} \quad (4)$$

where $\mu_N = e\hbar/(2M_p c)$ is the nuclear magneton and Q_Λ and μ_Λ are the electric charge and magnetic moment of the Λ baryon. We can see that the ratio has at least one zero at the origin, a consequence of the neutral charge on the Λ baryon.

Asymptotic behaviour In the perturbative-QCD framework, the asymptotic behavior for both the Sachs FFs is:

$$G_{E,M}^\Lambda(q^2) = O\left((q^2)^{-2}\right), \quad q^2 \rightarrow \infty, \quad (5)$$

given by the two gluons propagators appearing at the tree level of the interaction. The analyticity of the FFs implies that the Phragmén-Lindelöf theorem is applicable: by considering the bounded region between the positive and negative parts of the real axis in the complex plane, we can conclude that the FFs have the same asymptotic behaviour in the space-like and time-like regions, so that the power law obtained for the space-like region is valid also in the limit $q^2 \rightarrow \infty$. Since the two Sachs FFs share the same asymptotic power law, their ratio is indeed constant in the limit $|q^2| \rightarrow \infty$. As a consequence, the imaginary part of the time-like FFs ratio must tend to zero in the asymptotic limit.

In our case, in order to ensure the normalization at $q^2 = 0$ ($R(0) = 0$) and the asymptotic behavior of the FFs ratio $R(q^2)$, we must consider the one-time subtracted dispersion relation (DR)

for the real part, reconstructing the real and imaginary part of $R(q^2)$ on the upper edge of the real cut $(q_{\text{th}}^2, +\infty)$:

$$\begin{aligned} \text{Re}(f(x)) = & f(x_1) \\ & + \frac{x - x_1}{\pi} \text{Pr} \int_{x_0}^{\infty} \frac{\text{Im}(f(x'))}{(x' - x_1)(x' - x)} dx', \end{aligned} \quad (6)$$

where x_1 is the subtraction point in the real axis.

4. Parametrization and χ^2 definition

The imaginary part of the ratio is parametrized through a combination of Chebyshev polynomials of the first kind $T_j(x)$, with $j \in \mathbb{N} \cup \{0\}$ and $x \in [-1, 1]$, as described in [4]:

$$\begin{aligned} \text{Im}[R(q^2)] &\equiv Y(q^2; \vec{C}, q_{\text{asy}}^2) \\ Y(q^2; \vec{C}, q_{\text{asy}}^2) &= \begin{cases} \sum_{j=0}^N C_j T_j \left[x(q^2) \right], & q_{\text{th}}^2 < q^2 < q_{\text{asy}}^2, \\ 0, & q^2 \geq q_{\text{asy}}^2 \end{cases}, \end{aligned} \quad (7)$$

where $x(q^2) = 2(q^2 - q_{\text{th}}^2)/(q_{\text{asy}}^2 - q_{\text{th}}^2) - 1$.

This parametrization has $N + 2$ free parameters, the weights of the Chebyshev polynomials $\vec{C} = (C_0, C_1, \dots, C_N)$ and the asymptotic threshold q_{asy}^2 , where $\vec{C} \in \mathbb{R}^{N+1}$ and $q_{\text{asy}}^2 \in (q_{\text{phy}}^2, \infty)$. These parameters have to be determined by imposing theoretical and experimental constraints.

For the theoretical constraints, since the FF ratio is real at the theoretical, physical and asymptotic thresholds, the imaginary part $Y(q^2; \vec{C}, q_{\text{asy}}^2)$ must be equal to 0 at $q^2 = \{q_{\text{th}}^2, q_{\text{phy}}^2, q_{\text{asy}}^2\}$. This effectively reduces the number of degrees of freedom for the parametrization from $N + 2$ to $N - 1$. The theoretical constraints on the real part of the ratio set it equal to 1 at the physical threshold, and after the asymptotic threshold. Those constraints are inserted as additional terms in the χ^2 definition.

The experimental constraints are given by the data points of BaBar and BESIII experiments already mentioned in Sec 2. The χ^2 function is defined as

$$\begin{aligned} \chi^2(\vec{C}, q_{\text{asy}}^2) = & \chi_{|R|}^2 + \chi_{\phi}^2 \\ & + \tau_{\text{phy}} \chi_{\text{phy}}^2 + \tau_{\text{asy}} \chi_{\text{asy}}^2 + \tau_{\text{curv}} \chi_{\text{curv}}^2. \end{aligned} \quad (8)$$

The first two contributions are the definition of χ^2 for the data of the modulus and the phase respectively:

$$\chi_{|R|}^2 = \sum_{j=1}^M \left(\frac{\sqrt{X(q_j^2)^2 + Y(q_j^2)^2} - |R_j|}{\delta |R_j|} \right)^2, \quad (9)$$

$$\chi_{\phi}^2 = \sum_{k=1}^P \left(\frac{\sin(\arctan(Y(q_k^2)/X(q_k^2))) - \sin(\phi_k)}{\delta \sin(\phi_k)} \right)^2, \quad (10)$$

where we defined the real part of the ratio as $X(q^2)$, obtained through the dispersion relation as

$$X(q^2) \equiv \text{Re} \left(R(q^2) \right) = \frac{q^2}{\pi} \text{Pr} \int_{q_{\text{th}}^2}^{q_{\text{asy}}^2} \frac{Y(s)}{s(s - q^2)} ds. \quad (11)$$

The χ_{phy}^2 and χ_{asy}^2 contributions encode the constraints on the real part of the ratio at the physical and asymptotic threshold respectively:

$$\chi_{\text{phy}}^2 = \left(1 - X(q_{\text{phy}}^2) \right)^2, \quad \chi_{\text{asy}}^2 = \left(1 - X(q_{\text{asy}}^2) \right)^2. \quad (12)$$

The last term $\tau_{\text{curv}} \chi_{\text{curv}}^2$ is used to stabilize the solution of an ill-posed problem that includes the resolution of a Fredholm integral equation. This term minimizes the curvature of the integrated function $Y(q^2)$, in order to obtain less oscillating solutions, which arise naturally when dealing with integral equations. The final expression for χ_{curv}^2 is

$$\chi_{\text{curv}}^2 = \int_{q_{\text{th}}^2}^{q_{\text{asy}}^2} \left| \frac{d^2 Y(s)}{ds^2} \right|^2 ds. \quad (13)$$

It turns out that choosing τ_{phy} sufficiently big and τ_{asy} sufficiently small, the respective constraints are still exact, so two fixed values $\tau_{\text{phy,asy}}^0$ have been fixed at $\tau_{\text{phy}}^0 = 10^2$ and $\tau_{\text{asy}}^0 = 0$. For what regards the value of the regularization part, τ_{curv} , this allows the curvature of the imaginary part $Y(q^2; \vec{C}, q_{\text{asy}}^2)$ to be controlled during the minimization procedure. For this data set the best value of τ_{curv} turns out to be 0.05 [4]. From now on, we set the maximum Chebyshev polynomials' degree N to 5, since it minimizes the χ^2 for our experimental data.

5. Results and discussion

Since the imaginary part of the FFs at the theoretical and asymptotic thresholds is equal to 0, the value of the realtive phase $\arg(G_E^\Lambda/G_M^\Lambda)$ assumes a value equal to an integer of π radians, $N_{\text{th,asy}}$. The χ^2 minimization procedure, alongisde with a Monte Carlo variation on the data, allows the configurations of $(N_{\text{th}}, N_{\text{asy}})$ that better describe the experimental data associated with their probability of occurance to be determined.

Being Λ a neutral baryon, it is possbile to determine the mean electric-charge squared radius $\langle r_E^2 \rangle$ for each configuration as

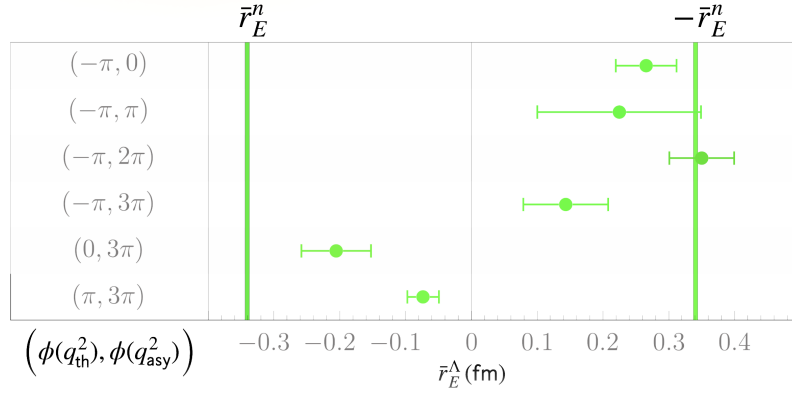
$$\langle r_E^2 \rangle = 6\mu_\Lambda \left. \frac{dR(q^2)}{dq^2} \right|_{q^2=0}. \quad (14)$$

which is indeed a function of the coefficients $\{\vec{C}, q_{\text{asy}}^2\}$.

The configurations' probabilities are reported in Table 1, while the charge radii are shown in Fig 1, where $\bar{r}_E^\Lambda = \text{Sgn}(\langle r_E^2 \rangle) \sqrt{\langle r_E^2 \rangle}$.

In conclusion, we can see that the most probable configuration $(N_{\text{th}}, N_{\text{asy}}) = (-1, 2)$ suggests a positive charge radius. We can give an heuristic interpretation in the sense that the negative charge, carried by the down and the heavy strange quarks, is mainly concentrated at small distances, in contrast with the neutron's behavior. Using the Levinson's theorem [5], we can also say, assuming the magnetic FF $G_M^\Lambda(q^2)$ has no zeroes in the complex plane, that the relative phase variance from

$(N_{\text{th}}, N_{\text{asy}})$	$P\{\%\}$
(-1,0)	4
(-1,1)	16
(-1,2)	50.5
(0,3)	26.8

Table 1: Probability of occurrence of each pair $(N_{\text{th}}, N_{\text{asy}})$ arising from the Monte Carlo procedure.**Figure 1:** Charge radii for each configuration $(N_{\text{th}}, N_{\text{asy}})$, where the symbol \bar{r}_E^n indicates the well known value assumed by the neutron.

the theoretical to the asymptotic thresholds divided by π gives the number of zero crossings in the complex plane of the function $R(q^2)$. The most probable value for this quantity is 3, hence there are 2 additional zeroes in the complex plane alongside the trivial one at $q^2 = 0$, given by the neutrality of the baryon.

References

- [1] Institute of High Energy Physics Chinese Academy of Sciences. Available at: <https://web.archive.org/web/20160316234203/http://www.ihep.ac.cn/english/E-Bepc/>.
- [2] B. Aubert et al., "Study of $e^+e^- \rightarrow \Lambda\bar{\Lambda}, \Lambda\bar{\Sigma}^0, \Sigma^0\bar{\Sigma}^0$ using initial state radiation with BABAR," Phys. Rev. D, vol. 76, no. 9, 092006, 2007. DOI: [10.1103/PhysRevD.76.092006](https://doi.org/10.1103/PhysRevD.76.092006).
- [3] M. Ablikim et al. (BESIII Collaboration), "Complete Measurement of the Λ Electromagnetic Form Factors," Phys. Rev. Lett., vol. 123, no. 12, 122003, 2019. DOI: [10.1103/PhysRevLett.123.122003](https://doi.org/10.1103/PhysRevLett.123.122003).
- [4] A. Mangoni, S. Pacetti, and E. Tomasi-Gustafsson, "First exploration of the physical Riemann surfaces of the ratio G_E^Λ/G_M^Λ ," Phys. Rev. D, vol. 104, no. 11, p. 116016, 2021.
- [5] N. Levinson, "On the uniqueness of the potential in a Schrödinger equation for a given asymptotic phase," Danske Vid. Selsk., Mat.-Fys. Medd., vol. 25, no. 9, 29 S., 1949. Zbl: [0032.20702](https://zbmath.org/?q=ser/0032.20702).